Chemical Engineering Journal 163 (2010) 236–242

Contents lists available at ScienceDirect

Chemical Engineering Journal

journal homepage: www.elsevier.com/locate/cej

Application of film-pore diffusion model for methylene blue adsorption onto plant leaf powders

V. Ponnusami*, K.S. Rajan, S.N. Srivastava

School of Chemical & Biotechnology, SASTRA University, Thanjavur, India

ARTICLE INFO

Article history:
Received 11 November 2009
Received in revised form 21 July 2010
Accepted 22 July 2010

Keywords:
Methylene blue
Adsorption kinetics
Film-pore diffusion model
Low-cost adsorbents

ABSTRACT

In the present work kinetics of methylene blue adsorption onto three low-cost adsorbents namely guava leaf powder (GLP), teak leaf powder (TLP) and gulmohar leaf powder (GUL) was predicted using film-pore diffusion model. The model equations were solved numerically by method of lines using Excel. Initial estimates of mass transfer parameters namely external-film transfer coefficient and internal diffusion coefficient were obtained using single resistance models at temperatures 303, 313 and 323 K and for initial dye concentrations 50, 100, 150 and 200 mg dm^{-3}. Film-pore diffusion model was then used to determine the concentration-independent values of these mass transfer coefficients. Thus, external-film transfer coefficients were found to be in the range of 3×10^{-6} to 35×10^{-6} m s^{-1}, 1×10^{-6} to 8×10^{-6} m s^{-1} and 1×10^{-6} to 11×10^{-6} m s^{-1} for guava, teak and gulmohar leaf powders, respectively, in the chosen temperature range. At the same time internal diffusion coefficients were in the range of 0.1×10^{-12} to 1.9×10^{-12} m^2 s^{-1}, 0.1×10^{-12} to 0.6×10^{-12} m^2 s^{-1} and 0.2×10^{-12} to 1.3×10^{-12} m^2 s^{-1} for guava, teak and gulmohar leaf powders, respectively. It was evident that film-pore diffusion model could satisfactorily describe kinetics of methylene blue adsorption onto the three low-cost adsorbents used.

1. Introduction

A wide variety of synthetic dyes are used in textile, plastic, leather and many other industries for coloring their products. A significant portion of the dyes remains unconsumed and, therefore, let out in the effluent. A recent survey indicates that on an average 150–200 l of water is consumed and about 125 l of effluent is generated per kg of finished textile produced in India. That is about one million liters of effluent is discharged per day by an average sized textile mill having a daily production of 8000 kg of finished products [1]. A substantial quantity of the dye used in textile mills is not fixed to fabric in dye baths; the degree of fixation is largely dependent on the type of dye used. The presence of dyes in aqueous effluents poses a serious ecological threat. It reduces light penetration in water bodies and interferes with metabolic activities of aquatic life [2]. Over the decades adsorption had been proven to be one of the efficient technologies among various physico-chemical methods available for the removal of dyes from aqueous effluents [3]. Since conventional adsorbents like activated carbon are very costly, identification of low-cost adsorbents would be very much beneficial to the community as a whole. Many researchers have, therefore, worked on this and have come up with potential low-cost adsorbents [4]. Recent studies include application of jackfruit peel [5], pine apple stem [6], phoenix tree leaves [7], pomelo peel [8], shells of bittim [9], orange peel [10], broad bean peels [11], etc.

In our previous reports we have established the feasibility and adsorption of MB onto three plant leaf powders namely guava leaf powder (GLP) [12], teak leaf powder (TLP) [13] and gulmohar leaf powder (GUL) [14]. For the design of adsorption system, adsorption capacity of the adsorbent and prediction of concentration decay curve are very much essential [15]. Adsorption capacity of these materials had been reported in our previous reports [12–14]. Identification of actual rate controlling step(s) enables efficient design of adsorption systems. Therefore, in the present work we have predicted the concentration decay curve for the abovementioned systems by employing film-pore diffusion model (FPDM). Using FPDM, external-film transfer coefficient and internal diffusion coefficients were evaluated and rate controlling step was identified.

2. Materials and methods

2.1. Materials

Methylene blue (MB, chemical formula: $C_{16}H_{18}N_3SCl$; FW: 320 g mol^{-1}, λ_{max} = 662 nm, class: thiazine, C.I. Classification Number: 52015) is one of the most important basic dyes used by textile

* Corresponding author at: SASTRA University, Department of Chemical Engineering, Thirumalaisamudram, Thanjavur, Tamil Nadu 613402, India.
Tel.: +91 4362 264101.
E-mail addresses: vponnu@chem.sastra.edu, ponnusamiv@yahoo.com (V. Ponnusami).

1385-8947/$ – see front matter © 2010 Elsevier B.V. All rights reserved.
doi:10.1016/j.cej.2010.07.052

Nomenclature

A_s	total surface area of all the particles ($m^2\,dm^{-3}$)
Bt	Biot number ($Bt = k_f d_p/D_{eff}$)
C_t	bulk concentration at time t ($mg\,dm^{-3}$)
C_s	surface concentration ($mg\,dm^{-3}$)
C_e	equilibrium dye concentration in liquid phase ($mg\,dm^{-3}$)
C_0	initial bulk concentration ($mg\,dm^{-3}$)
d_p	diameter of particle (m)
D_p	internal pore diffusivity ($m^2\,s^{-1}$)
D_{eff}	internal effective diffusivity ($m^2\,s^{-1}$)
K_L	Langmuir adsorption constant ($dm^3\,mg^{-1}$)
m_s	mass of particles added ($g\,dm^{-3}$)
r	radial position in the particle (m)
R	radius of the particle (m)
q_{avg}	average dye concentration in solid phase ($mg\,g^{-1}$)
q_e	solid phase dye concentration at equilibrium ($mg\,g^{-1}$)
q_i	solid phase dye concentration at grid i at time t ($mg\,g^{-1}$)
t	time (s or min)
V	volume of solution (dm^3)
ε	particle porosity
ρ_p	particle density ($kg\,m^{-3}$)
k_f	external-film transfer coefficient ($m\,s^{-1}$)
R^2	coefficient of determination
χ^2	chi square

industry. MB is preferentially adsorbed onto many solids. For this reason, MB was used in the present study. The MB dye was obtained from Ranbaxy Laboratories Limited (India) and used without further purification. MB is not regarded as acutely toxic, but it can have various harmful effects. On inhalation, it can give rise to short periods of rapid or difficult breathing, while ingestion through the mouth produces a burning sensation and may cause nausea, vomiting, diarrhea, and gastritis [5]. Guava, teak and gulmohar leaf powder samples were prepared as described in our earlier papers [12–14]. Procedure for stock solution preparation is described earlier in Ponnusami et al. [16].

2.2. Kinetic studies

Batch contact, sampling and concentration measurement were done as described in Ponnusami et al. [16]. Batch experiments were conducted at four different concentrations 50, 100, 150 and 200 $mg\,dm^{-3}$ and three temperatures 303, 313 and 323 K. Adsorbent dose, particle size, agitation speed used in the study were 2 $g\,dm^{-3}$, 125 μm and 200 RPM, respectively.

2.3. Kinetic models

From the mechanistic point of view sorption of dye is considered to involve following consecutive steps:

1. External diffusion of dye molecules across the liquid film surrounding the solid particles.
2. Adsorption of the solute on the adsorption site.
3. Internal diffusion of dye within the particle either by pore diffusion, surface diffusion or both.

Thus, adsorption kinetic models could be divided into two types, namely reaction-based models and diffusion based models [17,18]. Pseudo-first order [19] and pseudo-second order models [20–22] are the two most commonly used reaction-based kinetic models. However, as mentioned earlier for design of an efficient adsorption system it is necessary to predict mass transfer parameters namely external-film transfer coefficient and internal diffusion coefficient. Diffusion based models are useful for this purpose. Single resistance models were developed by assuming either external-film transfer [23] or internal mass transfer [24] as the sole rate controlling steps. These models help to get a quick estimate of mass transfer parameters. Two resistance models are more rigorous and allow estimation of mass transfer parameters more accurately. Film-pore diffusion [25], homogeneous surface diffusion [15], concentration dependent surface diffusion [26], and branched pore diffusion [27] models are such models available for the analysis of adsorption kinetics and are particularly useful when both the mass transfer steps are important. In FPDM it is assumed that the adsorbate first diffuses into the pores wherein dye molecules are adsorbed onto the internal surface of the adsorbents. The transport of adsorbate in liquids contained in the pores is assumed to follow Fick's law. Homogeneous solid diffusion model assumes that the dye molecules are adsorbed on the external surface of the adsorbents from where they diffuse through the solid towards the center of the particle. Both pore diffusion and solid diffusion are considered in combined diffusion model, while branched pore model takes into account the pore size distribution of the particle.

Analytical solutions are either not possible or very difficult for majority of these systems. Crank–Nicholson numerical method is most commonly used to solve the set of simultaneous partial differential equations defining the above models. Most recently orthogonal collocation method [28,29] had been applied for this kind of systems successfully. Crank–Nicholson implicit finite difference method, semi-analytical integration, and Cartesian collocation methods had been adopted and the results were compared by Lee and McKay [30].

In the present paper external-film diffusion model [23] and simplified Fickian diffusion model [24] are employed to predict external-film transfer coefficient and effective internal diffusion coefficient, respectively. Later these estimated values were used as initial guess values in solving FPDM.

2.3.1. External-film diffusion model

During the initial adsorption period only external diffusion resistance is predominant and controls the adsorption rate. Thus, during initial period of adsorption a simple external-film diffusion model can be developed by writing a mass balance for a batch adsorption system. In the development of the external-film diffusion model following assumptions are made:

1. Adsorbent particles are spherical.
2. Bulk concentration is uniform (perfect mixing).
3. During initial phase of adsorption, influence of internal diffusion resistance is negligible owing to negligible concentration in solid phase.
4. The rate of disappearance of adsorbate from the solution is equal to the rate of adsorption from the liquid phase to the outer surface of particle.
5. First order rate equation is applicable.

Therefore, the rate of adsorption can be written as:

$$\frac{dC}{dt} = -k_f \frac{A_s}{V}(C - C_s) \quad (1)$$

Integral solution of the Eq. (1) upon substituting the initial condition $C\big|_{t=0} = C_0 \& C_s\big|_{t=0} = 0$ is:

$$\ln \frac{C_t}{C_0} = -k_f \frac{A_s}{V} t \quad (2)$$

Thus, k_f can be determined from slope of the curve $\ln(C_t/C_0)$ versus t at time $t \to 0$ [23].

2.3.2. Fickian diffusion model

Similarly, effective internal diffusivity can be calculated using simplified Fickian diffusion equation [24,31,32]. For longer duration of contact times (when t is large) it is given by the following expression:

$$\ln\left(1 - \frac{q_t}{q_e}\right) = \ln\frac{6}{\pi^2} - k't \tag{3}$$

where $k' = (D_p\pi^2)/R^2$.

Internal pore diffusivity D_p can be calculated, using Eq. (3), by making a plot of $\ln(1 - q_t/q_e)$ versus time.

2.3.3. Film-pore diffusion model

In the present work FPDM is used to predict concentration decay curve. This model takes into account both external film and internal resistances. Thus, the governing model includes the following expressions:

2.3.3.1. External mass transfer. The rate of mass transfer in the external film surrounding the solid particle is assumed to be directly proportional to the concentration difference in the film. Therefore,

$$\frac{dC_t}{dt} = -k_f\frac{A_s}{V}(C_t - C_s) \tag{4}$$

2.3.3.2. Pore diffusion. Mass transfer in the liquid inside the pore should follow Fick's law of diffusion. Writing a material balance equation for adsorption of dye with pore diffusion, in a spherical particle, the following equation is obtained:

$$\varepsilon\frac{\partial C_i}{\partial t} + \rho_p\frac{\partial q_i}{\partial t} = D_{eff}\left[\frac{\partial^2 C_i}{\partial r^2} + \frac{1}{r}\frac{\partial C_i}{\partial r}\right] \tag{5}$$

The initial condition is expressed as

$$\text{At}\quad t = 0, \quad C_i = 0 \quad \text{for}\quad 0 \le r \le R \tag{6}$$

The boundary condition at the center of the particle (called symmetry condition) is expressed as:

$$\frac{\partial C_i}{\partial r} = 0 \quad \text{at}\quad r = 0 \tag{7}$$

At the solid surface, the rate at which the solute is transferred through the external film must be equal to the rate at which it diffuses into the solid. Thus, the second boundary condition could be written at the surface of the particle as follows:

$$k_f(C_t - C_s) = D_{eff}\left.\frac{\partial C_i}{\partial r}\right|_{r=R} \tag{8}$$

2.3.3.3. Equilibrium. Spontaneous equilibrium is assumed in the liquid–solid interface within the pores. Therefore, solid phase concentration at any radial location and time can be related to the aqueous phase concentration by the isotherm equation expressed as:

$$q_i = f(C_i) \tag{9}$$

Substituting Eq. (9) in Eq. (5) we get:

$$\varepsilon\frac{\partial C_i}{\partial t} + \rho_p\frac{\partial f(C_i)}{\partial t} = D_{eff}\left[\frac{\partial^2 C_i}{\partial r^2} + \frac{1}{r}\frac{\partial C_i}{\partial r}\right] \tag{10}$$

Since Langmuir isotherm explained the equilibrium well [12–14] for these systems Eq. (9) can be written as:

$$q_i = f(C_i) = \frac{q_e K_L C_i}{1 + K_L C_i} \tag{11}$$

2.3.3.4. Average dye concentration in the solid phase. Average particle concentration is obtained using the following integral

$$q_{avg} = \left(\frac{3}{R^3}\right)\int_0^R qr^2\,dr \tag{12}$$

2.3.3.5. Overall mass balance. Making solute balance for the adsorption reactor as a whole, liquid phase concentration can be obtained from the following expression:

$$V\frac{dC_t}{dt} = m_s\frac{dq_{avg}}{dt} \tag{13}$$

Corresponding initial conditions are:

$$\text{At}\quad t = 0, \quad C_t = C_0 \quad \text{and}\quad q_{avg} = 0 \tag{14}$$

In order to convert the equations to dimensionless form following dimensionless variables are defined,

$$Z = \frac{r}{R};\quad \overline{C_i} = \frac{C_i}{C_0};\quad \overline{C_t} = \frac{C_t}{C_0};\quad B_i = \frac{k_f R}{D_{eff}};\Bigg\} \tag{15}$$

Eq. (10) can be rewritten as follows:

$$\frac{\partial\overline{C_i}}{\partial\tau} = A(\overline{C_i})\left[\frac{\partial^2\overline{C_i}}{\partial Z^2} + \frac{1}{Z}\frac{\partial\overline{C_i}}{\partial Z}\right] \tag{16}$$

where

$$A(\overline{C_i}) = \frac{1}{\{\varepsilon + (q_h\rho_p/C_0)(1 + bC_0/(1 + bC_0\overline{C_i})^2)\}} \tag{17}$$

Then, the modified initial and boundary conditions become:

$$\left.\overline{C_i}\right|_{\tau=0} = 0 \quad \text{for}\quad 0 \le Z \le 1 \tag{18}$$

$$\left.\frac{\partial\overline{C_i}}{\partial\tau}\right|_{Z=0} = 0, \quad \text{for}\quad \tau \ge 0 \tag{19}$$

$$B_i(\overline{C_t} - \overline{C_s}) = \left.\frac{\partial\overline{C_i}}{\partial Z}\right|_{Z=1} \tag{20}$$

Modified integral for dimensionless average concentration in the solid phase is:

$$\overline{q_{avg}} = 3\int_0^1 \overline{q}Z^2\,dZ \tag{21}$$

The overall mass balance for solute becomes:

$$\frac{d\overline{C_t}}{d\tau} = \frac{m_s q_h}{VC_{b0}}\frac{d\overline{q_{avg}}}{d\tau} \tag{22}$$

Corresponding initial conditions are:

$$\left.\overline{C_t}\right|_{\tau=0} = \overline{C_0};\quad \text{and}\quad \left.\overline{q_{avg}}\right|_{\tau=0} = 0 \tag{23}$$

Eqs. (16)–(23) are solved numerically by method of lines. The governing PDEs coupled with their boundary conditions were transformed into a set of first order ODEs. The radial derivatives were discretized using central finite difference method. A computer program employing forward time progression was setup in Excel 2003 to yield a time trend of bulk liquid phase concentration. Single external mass transfer coefficient and single effective diffusion coefficients were determined so as to minimize the error between

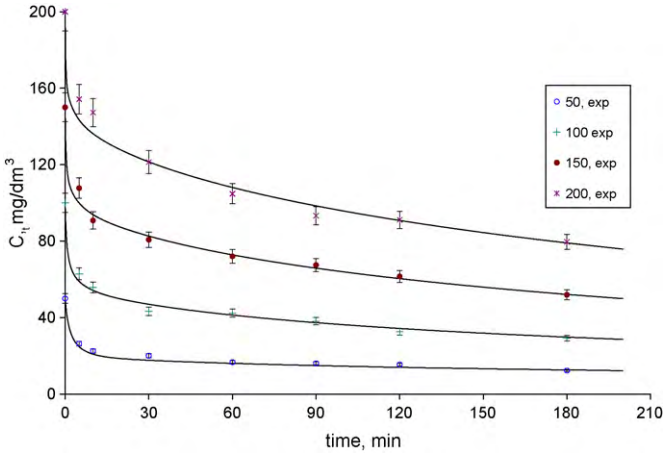

Fig. 1. Concentration decay curve: effect of initial concentration on adsorption of MB onto GLP (T = 303 K, RPM = 200; dosage = 2 g dm^{-3}; particle size = 125 μm, solid lines show predicted concentration decay curves, error bars show ±10% deviation).

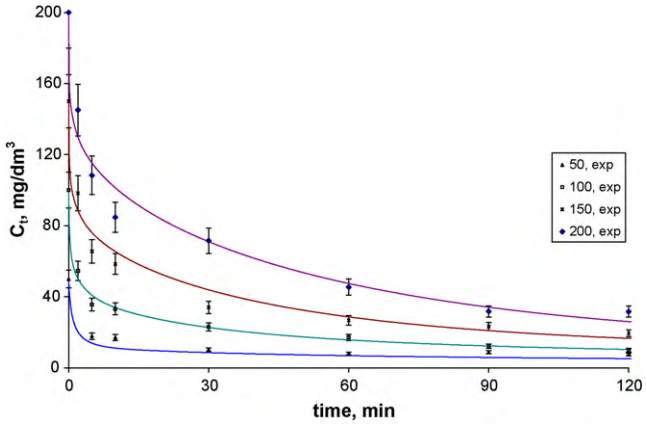

Fig. 2. Concentration decay curve: effect of initial concentration on adsorption of MB onto GLP (T = 313 K, RPM = 200; dosage = 2 g dm^{-3}; particle size = 125 μm, solid lines show predicted concentration decay curves, error bars show ±10% deviation).

the experimental data and predicted data. Chi square define below was used as a measure of error [33].

$$\chi^2 = \sqrt{\frac{q_{exp}^2 - q_t^2}{q_t}} \quad (24)$$

3. Results and discussion

External-film coefficient and internal pore diffusivities were determined using Eqs. (2) and (3). Results are given in Table 1.

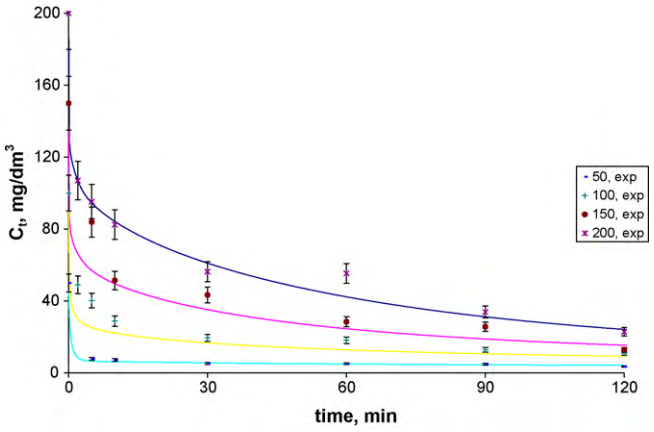

Fig. 3. Concentration decay curve: effect of initial concentration on adsorption of MB onto GLP (T = 323 K, RPM = 200; dosage = 2 g dm^{-3}; particle size = 125 μm, solid lines show predicted concentration decay curves, error bars show ±10% deviation).

Table 1
Effect of concentration and temperature on mass transfer coefficients for adsorption of MB onto GLP, TLP and GUL obtained using single resistance models (D = 2 g dm^{-3}, RPM = 200, d_p = 125 μm).

T (K)	C_0 (mg dm^{-3})	$k_f \times 10^6$ (m s^{-1})			$D_{eff} \times 10^{12}$ (m^2 s^{-1})		
		GLP	TLP	GUL	GLP	TLP	GUL
303	50	8.06	2.378	3.18	0.155	0.554	0.672
	100	6.16	2.015	2.83	0.596	0.382	0.283
	150	4.46	1.831	2.52	0.584	0.359	0.444
	200	3.29	1.447	2.08	0.417	0.303	0.264
313	50	11.73	3.971	2.56	0.745	0.312	0.388
	100	9.49	3.513	2.24	0.728	0.401	0.334
	150	8.10	2.840	1.96	0.510	0.366	0.270
	200	6.11	2.407	1.76	0.670	0.187	0.249
323	50	35.98	7.648	10.15	0.364	0.266	1.119
	100	11.30	7.136	9.22	0.976	0.412	1.204
	150	7.10	6.970	6.28	0.990	0.169	0.685
	200	9.12	6.170	4.77	1.816	0.426	0.572

External-film transfer coefficients were found to be in the range of 3×10^{-6} to 35×10^{-6} m s^{-1}, 1×10^{-6} to 8×10^{-6} m s^{-1} and 1×10^{-6} to 11×10^{-6} m s^{-1} for guava, teak and gulmohar leaf powders, respectively. Meantime internal diffusion coefficients were in the range of 0.1×10^{-12} to 1.9×10^{-12} m^2 s^{-1}, 0.1×10^{-12} to 0.6×10^{-12} m^2 s^{-1} and 0.2×10^{-12} to $1.3 \times 10^{-12} \times$ m^2 s^{-1} for guava, teak and gulmohar leaf powders. As mentioned earlier these single resistance models are oversimplified. External-film resistance model neglects internal resistance and is applicable during initial period only. It had been indicated in the published literature that external-film resistance model is applicable when contact time

Table 2
Mass transfer coefficients obtained using film-pore diffusion model (adsorption of MB onto GLP).

Temperature (K)	C_0 (mg dm^{-3})	k_f (m s^{-1})	D_{eff} (m^2 s^{-1})	R^2	χ^2	B_i
303	50	1.00×10^{-6}	1.74×10^{-13}	0.977	0.8	717
	100			0.970	0.7	
	150			0.967	0.8	
	200			0.977	2.1	
313	50	1.71×10^{-6}	6.46×10^{-13}	0.911	7.3	331
	100			0.981	0.8	
	150			0.978	5.3	
	200			0.974	4.6	
323	50	4.27×10^{-6}	3.11×10^{-13}	0.771	2.3	1716
	100			0.943	14.3	
	150			0.911	18.1	
	200			0.994	8.9	

Table 3
Mass transfer parameters for adsorption of MB onto TLP.

Temperature (K)	C_0 (mg dm^{-3})	k_f (m s^{-1})	D_{eff} (m^2 s^{-1})	R^2	χ^2	B_i
303	50	1.70×10^{-6}	7.2×10^{-13}	0.982	3.9	295
	100			0.993	0.9	
	150			0.993	2.5	
	200			0.989	1.9	
313	50	4.42×10^{-6}	4.0×10^{-12}	0.996	0.49	139
	100			0.995	1.38	
	150			0.997	1.93	
	200			0.997	0.49	
323	50	3.00×10^{-5}	1.9×10^{-11}	0.998	4.0	194
	100			0.997	1.6	
	150			0.980	0.7	
	200			0.992	1.4	

is less than 25 min [18]. Similarly during later period of adsorption effect of external film gradually decreases and pore resistance becomes more predominant. Because of these reasons more often these models predicts external-film transfer coefficient and internal pore diffusivity as a function of initial dye concentration. The results shown only exhibit this. However, for more accurate results both these resistances must be considered and hence in the present study film-pore diffusion model had been used. Concentration-independent external-film transfer coefficient and the internal diffusion coefficients were calculated using numerical method outlined earlier in Section 2.3. Microsoft Excel 2003 was used to solve the FPDM. Solver add-in was used to find the optimum values of film transfer coefficient and internal diffusion coefficient that would minimize an objective error function defined vide Eq. (24). Particle size, initial concentration, adsorbent dosage, Langmuir isotherm constants, number of grid points for radial coordinate and number of time steps were provided as inputs to the program. Film transfer coefficient and internal diffusion coefficients obtained by single resistance models were then supplied to the program as initial guess. For each set of data, χ^2 values were calculated for all the four concentrations used in the study (50, 100, 150 and 200 mg dm^{-3}). Sum of these χ^2 was then calculated for a given temperature. Values of k_f and D_{eff} were then iterated, using Solver add-in of Excel 2003, in such a way that sum of χ^2 was minimized. The values of concentration-independent external-film transfer coefficients and internal pore diffusivities that minimized the sum of χ^2 values were obtained at 303, 313 and 323 K. The results are listed in Table 2 along with corresponding values of R^2, χ^2 and Biot numbers for the adsorption of MB onto GLP under different temperatures and initial concentrations. High values of R^2 (close to 1) and low values of χ^2 indicate the suitability of film-pore diffusion model for the adsorption of MB onto GLP. Figs. 1–3 illustrate excellent agreement between predicted decay curves and experimental concentration decay data for the adsorption of MB onto GLP at temperatures 303, 313 and 323 K. Thus, it was established that FPDM could predict the concentration decay curves, with concentration-independent k_f and D_{eff} for a given temperature. However, at low concentrations the predicted curve did deviate slightly from the experimental data. This could be attributed to the fact that surface diffusion played a significant role in controlling the overall adsorption process when the initial concentration was low. Values of Biot numbers were significantly large (>100) indicating that internal diffusion was the rate controlling step for adsorption MB onto GLP [34].

Similarly, film transfer coefficients and effective internal diffusivities were determined using FPDM for the adsorption of MB onto teak and gulmohar leaf powders. These values are listed in Tables 3 and 4 along with corresponding R^2 and χ^2 values. Comparisons of predicted concentration decay curve with experimental data at 303, 313 and 323 K for these systems are shown in Figs. 4–9. It was evident from these figures that there was a good agreement between experimental data and predicted curves. Adsorptions of MB onto guava, teak and gulmohar leaf powders were all found to be controlled by internal pore resistance.

In all these cases k_f was found to increase with increase in solution temperature. Higher the solution temperature, greater was the mobility of the solutes. Also increase in temperature probably resulted in decrease in boundary layer thickness and decrease in solution viscosity. Relationship between temperature and k_f could be expressed empirically by the following expressions:

$$\text{GLP}: \quad k_f = 7 \times 10^{-11} T^{2.8}, \quad R^2 = 0.9514 \tag{25}$$

$$\text{GUL}: \quad k_f = 5 \times 10^{-08} T^{1.5}, \quad R^2 = 0.9968 \tag{26}$$

$$\text{TLP}: \quad k_f = 1 \times 10^{-14} T^{5.5}, \quad R^2 = 0.9322 \tag{27}$$

In empirical correlations T is substituted in °C.

It could be noticed that in all these experiments the rate of MB uptake by guava, teak and gulmohar leaf powders was rapid during first few minutes. This could be obviously

Table 4
Mass transfer coefficients for adsorption of MB onto GUL.

Temperature (K)	C_0 (mg dm^{-3})	k_f (m s^{-1})	D_{eff} (m^2 s^{-1})	R^2	χ^2	B_i
303	50	1.00×10^{-5}	1.8×10^{-12}	0.993	1.428	710
	100			0.992	4.085	
	150			0.991	2.350	
	200			0.994	2.508	
313	50	1.50×10^{-5}	9×10^{-13}	0.992	0.554	2083
	100			0.995	0.643	
	150			0.997	0.336	
	200			0.998	0.735	
323	50	2.2×10^{-5}	7×10^{-12}	0.993	6.661	393
	100			0.983	4.231	
	150			0.988	1.719	
	200			0.986	5.865	

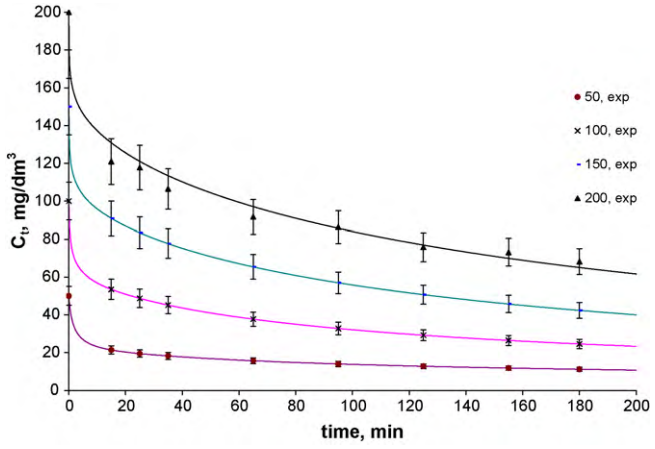

Fig. 4. Concentration decay curve: effect of initial concentration on adsorption of MB onto TLP (T = 303 K, RPM = 200; dosage = 2 g dm^{-3}; particle size = 125 μm, solid lines show predicted concentration decay curves, error bars show ±10% deviation).

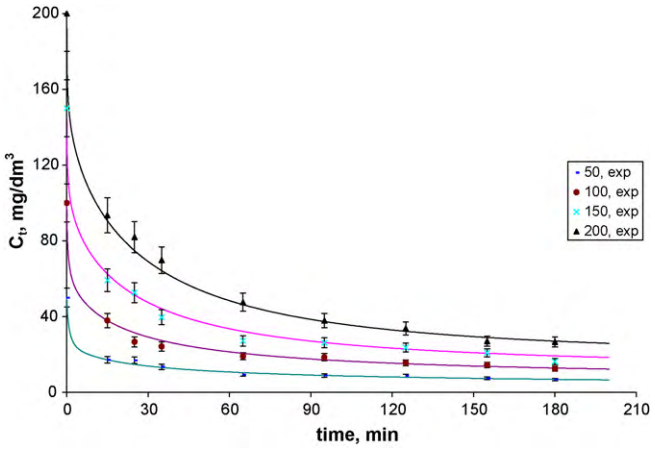

Fig. 5. Concentration decay curve: effect of initial concentration on adsorption of MB onto TLP (T = 313 K, RPM = 200; dosage = 2 g dm^{-3}; particle size = 125 μm, solid lines show predicted concentration decay curves, error bars show ±10% deviation).

attributed to the increased driving force (difference between the chemical potential of MB in aqueous and solid phases) for mass transfer during initial stages of adsorption (high bulk concentration and low solid phase concentration). It may, therefore, be beneficial to go for multi-stage counter current contact.

Internal pore diffusivities were found to be in the range of 10^{-11} to 10^{-13} m^2 s^{-1}. The orders of magnitude of pore diffusivities were consistent with those reported by previous researchers [27,35]. Physico-chemical properties of the solutes like size, polarity and solubility may affect the magnitude of the pore diffusivities [36,37].

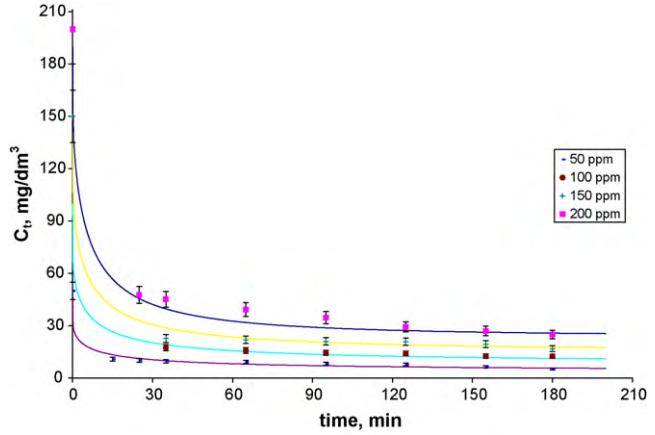

Fig. 6. Concentration decay curve: effect of initial concentration on adsorption of MB onto TLP (T = 323 K, RPM = 200; dosage = 2 g dm^{-3}; particle size = 125 μm, solid lines show predicted concentration decay curves, error bars show ±10% deviation).

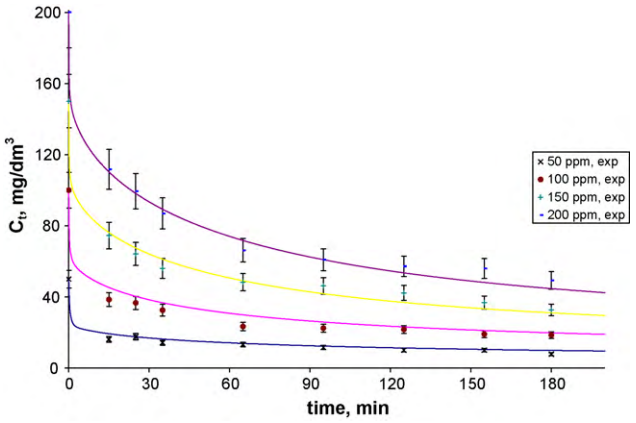

Fig. 7. Concentration decay curve: effect of initial concentration on adsorption of MB onto GUL (T = 303 K, RPM = 200; dosage = 2 g dm^{-3}; particle size = 125 μm, solid lines show predicted concentration decay curves, error bars show ±10% deviation).

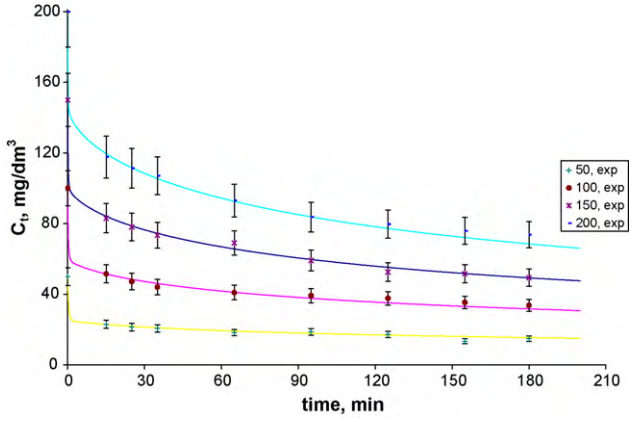

Fig. 8. Concentration decay curve: effect of initial concentration on adsorption of MB onto GUL (T = 313 K, RPM = 200; dosage = 2 g dm^{-3}; particle size = 125 μm, solid lines show predicted concentration decay curves, error bars show ±10% deviation).

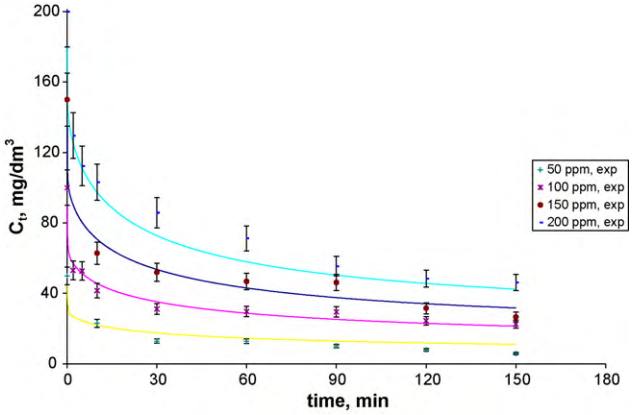

Fig. 9. Concentration decay curve: effect of initial concentration on adsorption of MB onto GUL (T = 323 K, RPM = 200; dosage = 2 g dm^{-3}; PARTICLE size = 125 μm, solid lines show predicted concentration decay curves, error bars show ±10% deviation).

MB is in fact a bulky molecule. Molecular diameter of MB molecule is about 0.8 nm [38]. Pore diffusivities were lower probably due to large size of MB molecules.

4. Conclusion

In the present paper applicability of FPDM for prediction of concentration decay curve for adsorption of MB onto guava, teak and gulmohar leaf powders was investigated. It was found that the model could predict the concentration decay curve for all the three system excellently with a small deviation during initial period. The model was able to predict single value of external-film transfer coefficient and single value of internal diffusion coefficient which are independent of initial dye concentration. External-film transfer coefficients were in the order of 10^{-6} m s^{-1} and internal diffusion coefficients were in the order of 10^{-12} m^2 s^{-1} for all the three systems. Based on the values of Biot number it was concluded that MB adsorption onto guava, teak and gulmohar leaf powders were controlled by internal pore resistance. It was also noticed that external-film coefficient increased with increase in temperature.

References

[1] S. Bhogle, Case study on wastewater disposal practices and likely treatment options, in: Textile Processing Units in Tamilnadu, TIDE, Bangalore, 2007.
[2] N. Yeddou, A. Bensmalli, Kinetic models for the sorption of dye from aqueous solution by claywood sawdust mixture, Desalination 185 (2005) 499–508.
[3] J.C. Morris, W.J. Weber Jr., Preliminary Appraisal of Advanced Waste Treatment Processes, Public Health Service Publication, 1962, pp. W62–W64.
[4] A. Bhatnagar, M. Sillanpää, Utilization of agro-industrial and municipal waste materials as potential adsorbents for water treatment—a review, Chem. Eng. J. 157 (2010) 277–296.
[5] B.H. Hameed, Removal of cationic dye from aqueous solution using jackfruit peel as non-conventional low-cost adsorbent, J. Hazard. Mater. 162 (2009) 344–350.
[6] B.H. Hameed, R.R. Krishni, S.A. Sata, A novel agricultural waste adsorbent for the removal of cationic dye from aqueous solutions, J. Hazard. Mater. 162 (2009) 305–311.
[7] R. Han, W. Zou, W. Yu, S. Cheng, Y. Wang, J. Shi, Biosorption of methylene blue from aqueous solution by fallen phoenix tree's leaves, J. Hazard. Mater. 141 (2007) 156–162.
[8] B.H. Hameed, D.K. Mahmoud, A.L. Ahmad, Sorption of basic dye from aqueous solution by pomelo (*Citrus grandis*) peel in a batch system, Colliod Surf. A: Physicochem. Eng. Aspects 316 (2008) 78–84.
[9] H. Aydin, G. Baysal, Adsorption of acid dyes in aqueous solutions by shells of bittim (*Pistacia khinjuk* stocks), Desalination 196 (2006) 248–259.
[10] F. Doulati Ardejani, Kh. Badii, N. Yousefi Limaee, N.M. Mahmoodi, M. Arami, S.Z. Shafaei, A.R. Mirhabibi, Numerical modelling and laboratory studies on the removal of Direct Red 23 and Direct Red 80 dyes from textile effluents using orange peel, a low-cost adsorbent, Dyes Pigments 73 (2007) 178–185.
[11] B.H Hameed, M.I. El-Khaiary, Sorption kinetics and isotherm studies of a cationic dye using agricultural waste: broad bean peels, J. Hazard. Mater. 154 (2008) 639–648.
[12] V. Ponnusami, S. Vikram, S.N. Srivastava, Guava (*Psidium guajava*) leaf powder: novel adsorbent for removal of methylene blue from aqueous solutions, J. Hazard. Mater. 152 (2008) 276–286.
[13] V. Ponnusami, S.N. Srivastava, Studies on application of teak leaf powders for the removal of color from synthetic and industrial effluents, J. Hazard. Mater. 169 (2009) 1159–1162.
[14] V. Ponnusami, V. Gunasekar, S.N. Srivastava, Kinetics of methylene blue removal from aqueous solution using gulmohar (*Delonix regia*) plant leaf powder: multivariate regression analysis, J. Hazard. Mater. 169 (2009) 119–127.
[15] B. Al Duri, G. Mckay, Basic dye adsorption on carbon using a solid-phase diffusion model, Chem. Eng. J. 38 (1988) 23–31.
[16] V. Ponnusami, V. Krithika, R. Madhuram, S.N. Srivastava, Effects of process variables on kinetics of methylene blue sorption onto untreated guava (*Psidium Guajava*) leaf powder: statistical analysis, Chem. Eng. J. 140 (2008) 609–613.
[17] Y.S. Ho, J.C.Y. Ng, G. McKay, Kinetics of pollutant sorption by biosorbents: review, Sep. Purif. Methods 29 (2000) 189–232.
[18] Y.S. Al-Degs, M.I. El-Barghouthi, A.A. Issa, M.A. Khraisheh, G.M. Walker, Sorption of Zn(II), Pb(II), and Co(II) using natural sorbents: equilibrium and kinetic studies, Water Res. 40 (2006) 2645–2658.
[19] S. Lagergren, Zur theorie der sogenannten adsorption gelo¨ster stoffe, Kungliga Svenska Vetenskapsakademiens, Handlingar 24 (1898) 1–39.
[20] Y.S. Ho, G. McKay, The kinetics of sorption of divalent metal ions onto sphagnum moss peat, Water Res. 34 (2000) 735–742.
[21] Y.S. Ho, G. McKay, Pseudo-second order model for sorption processes, Process. Biochem. 34 (1999) 451–465.
[22] Y.S. Ho, G. McKay, Sorption of dye from aqueous solution by peat, Chem. Eng. J. 70 (1998) 115–124.
[23] S. Dutta, J.K. Basu, R.N. Ghar, Studies on adsorption of p-nitrophenol on charred saw-dust, Sep. Purif. Technol. 21 (2001) 227–235.
[24] Y. Onal, C. Akmil-Basar, C. Sarici-Ozdemir, Investigation kinetics mechanisms of adsorption malachite green onto activated carbon, J. Hazard. Mater. 146 (2007) 194–203.
[25] G. McKay, B. Al-Duri, Study of the mechanism of pore diffusion in batch adsorption systems, J. Chem. Technol. Biotechnol. 48 (1990) 269–285.
[26] T.S.Y. Choong, T.N. Wong, T.G. Chuah, A. Idris, Film-pore-concentration-dependent surface diffusion model for the adsorption of dye onto palm kernel shell activated carbon, J. Colloid Interface Sci. 301 (2006) 436–440.
[27] D.C.K. Ko, J.F. Porter, G. McKay, A branched pore model analysis for the adsorption of acid dyes on activated carbon, Adsorption 8 (2002) 171–188.
[28] A.I. Liapis, D.W.T. Rippin, A general model for the simulation of multicomponent adsorption from a finite bath, Chem. Eng. Sci. 32 (1977) 619–627.
[29] G. McKay, Solution to the homogeneous surface diffusion model for batch adsorption systems using orthogonal collocation, Chem. Eng. J. 81 (2001) 213–221.
[30] V.K.C. Lee, G. McKay, Comparison of solutions for the homogeneous surface diffusion model applied to adsorption systems, Chem. Eng. J. 98 (2004) 255–264.
[31] G.M. Walker, L. Hansen, J.-A. Hanna, S.J. Allen, Kinetics of a reactive dye adsorption onto dolomitic sorbents, Water Res. 37 (2003) 2081–2089.
[32] J. Crank, The Mathematics of Diffusion, 2nd ed., Clarendon Press, Oxford, 1975.
[33] Y.-S. Ho, W.-T. Chiu, C.-C. Wang, Regression analysis for the sorption isotherms of basic dyes on sugarcane dust, Bioresour. Technol. 96 (2005) 1285–1291.
[34] H. Wu, S. Wang, H. Kong, W. He, M. Xia, Determination of bulk mass transfer coefficient of biosorption on sludge granule based on liquid membrane mass transfer mechanism, Bioresour. Technol. 98 (2007) 2953–2957.
[35] K.K.H. Choy, J.F. Porter, G. McKay, A film-pore-surface diffusion model for the adsorption of acid dyes on activated carbon, Adsorption 7 (2001) 305–317.
[36] F.-C. Wu, R.-L. Tseng, R.-S. Juang, Initial behavior of intraparticle diffusion model used in the description of adsorption kinetics, Chem. Eng. J. 153 (2009) 1–8.
[37] F.-C. Wu, R.-L. Tseng, S.-C. Huang, R.-S. Juang, Characteristics of pseudo-second-order kinetic model for liquid-phase adsorption: a mini-review, Chem. Eng. J. 151 (2009) 1–9.
[38] J. Zhang, K.H. Lee, L. Cui, T. Jeong, Degradation of methylene blue in aqueous solution by ozone-based processes, J. Ind. Eng. Chem. 15 (2009) 185–189.